

Virtual Photon Structure from Low Q^2 Jet Production¹

G. Kramer, B. Pötter

*II. Institut für Theoretische Physik,² Universität Hamburg,
Luruper Chaussee 149, D-22761 Hamburg, Germany
E-mail: kramer@mail.desy.de, poetter@mail.desy.de*

Abstract

We review next-to-leading order calculations of one- and two-jet production in ep collisions at HERA for photon virtualities in the range $1 < Q^2 < 100$ GeV². Soft and collinear singularities are extracted using the phase space slicing method. Numerical results are presented for HERA conditions with the Snowmass jet definition. The transition between photoproduction and deep-inelastic scattering is studied. We discuss the comparison with recent H1 data of the dijet rate and differential dijet cross sections with special attention to the region, in which two jets have equal transverse momenta.

1 Introduction

The interaction of the virtual photon with the constituents of the proton in high energy ep collisions is described differently depending how large the scale of the photon virtuality Q^2 is. For large Q^2 , i.e. large compared to other kinematical variables, as for example the E_T^2 of produced jets, the virtual photon couples only directly to the quarks originating from the proton. In the region $0 \lesssim Q^2 \lesssim Q_{max}^2$ with Q_{max}^2 being small, the virtual photon couples either directly to a parton from the proton (so-called direct process) or through resolved processes, in which the photon transforms into partons and one of these interacts with a parton out of the proton to produce jets. On this basis the theory for photoproduction ($Q^2 \simeq 0$) of jets at HERA and LEP, i.e. in γp and $\gamma\gamma$ processes, has been developed up to next-to-leading order (NLO) QCD [1] and good agreement with the experimental data from HERA and LEP has been found [2]. The cross section for jet production is expressed as a convolution of universal parton distributions (PDF's) of the proton and, in the resolved case, of the photon with the hard parton-parton scattering cross section. The evolution of both parton densities with the scale μ as well as the hard parton-parton

¹To appear in the proceedings of the workshop on photon interactions and the photon structure, in Lund, September 1998

²Supported by Bundesministerium für Forschung und Technologie, Bonn, Germany, under Contract 05 7 HH 92P (0), and by EU Fourth Framework Program *Training and Mobility of Researchers* through Network *Quantum Chromodynamics and Deep Structure of Elementary Particles* under Contract FMRX-CT98-0194 (DG12 MIHT).

scattering cross section can be calculated in perturbative QCD as long as the scale μ of the hard subprocess, which is of the order of the transverse energy E_T of the produced jets, is large enough as compared to Λ_{QCD} and to Q . For these processes the photon densities are defined for photon virtualities $Q^2 = 0$ and are constructed in such a way as to describe the wealth of data in deep-inelastic $e\gamma$ scattering or $\gamma^*\gamma$ scattering, where the photon γ^* has a large virtuality.

For large $Q^2 \gg E_T^2$, i.e. in the deep inelastic region, the resolved process is supposed to be absent and the hard electron-proton scattering cross section expanded in powers of α_s has to be convoluted only with the known PDF's of the proton. In this region jet production has been calculated with the help of several programs [3] and compared to data from the H1 and ZEUS collaborations [4] for various Q^2 regions.

Thus we have a reasonably well tested theory for the photoproduction region, i.e. regions of Q^2 which includes $Q^2 \simeq 0$, and the deep inelastic region, where Q^2 is the large scale. Then the problem arises, how to calculate jet production in ep collisions with a fixed $Q^2 \neq 0$, although small compared to or at least less than the hard scattering scale μ^2 ($Q^2 \lesssim \mu^2$), which is usually taken to be of the order of E_T^2 . This challenging region of intermediate photon virtuality, where we have a typical two-scale problem, has been considered by several authors in leading order (LO) [5, 6, 7] and in NLO by us together with M. Klasen [8] and very recently in [9]. In the meantime the results of several analyses of H1 [10, 11, 12, 13] and ZEUS [14] measurements of jet production in various ranges of non-vanishing Q^2 , namely $0.2 < Q^2 < 4 \text{ GeV}^2$ [14], $1.4 < Q^2 < 25 \text{ GeV}^2$ [12], $1.6 < Q^2 < 80 \text{ GeV}^2$ [11] and $5 < Q^2 < 100 \text{ GeV}^2$ [13] have been published or presented at workshops.

As long as the non-vanishing $Q^2 \ll \mu^2$, it is justified for calculating jet production to introduce a resolved contribution in addition to the direct contribution in the same way as it has been done in the real photoproduction case. Then the parton distributions of the photon depend on x and the scale μ^2 , as in real photoproduction ($Q^2 = 0$), and in addition on the virtuality Q^2 . Several models exist for describing the μ^2 evolution of these parton distribution functions (PDF's) with changing Q^2 [5, 15, 16], but very little data from deep-inelastic $e\gamma^*$ scattering with photons γ^* of virtuality $Q^2 \neq 0$ [17] exist, where they could be tested. Experimental data from jet production in the region $Q^2 \ll \mu^2 \sim E_T^2$ could help to gain information on the Q^2 evolution of these photon structure functions. Parton densities of the virtual photon are suppressed [5, 15, 18] with increasing Q^2 and are, in the usual LO definition, assumed to vanish like $\ln(\mu^2/Q^2)$ for $Q^2 \rightarrow \mu^2$, so that in the region $Q^2 \sim \mu^2$ the direct process dominates. Therefore, in the LO framework, it depends very much on the choice of scale μ^2 in relation to E_T^2 , whether a resolved contribution is present in the region $Q^2 \geq E_T^2$. This leads to a large scale dependence in addition to the usual scale dependence of LO predictions and a treatment up to NLO is called for. In analogy to the photoproduction case in NLO the resolved and the direct contributions are related to each other. So, if one adds for $Q^2 \neq 0$ a resolved contribution, this has to be done in such a way that the contributions involving the PDF's of the virtual photon are matched with the NLO direct photon contributions by subtracting from the latter those terms which are already included through the PDF's of the virtual photon. Such a subtraction has been worked out in our earlier work with M. Klasen [9] by separating the collinear photon initial state singularities from the NLO corrections to the direct cross section. There we studied inclusive one- and two-jet production with virtual photons in the region $Q^2 \ll E_T^2$ by transforming to the HERA laboratory system. In this system the results were compared to the photoproduction cross sections and the unsubtracted direct-photon

cross section up to NLO. The dependence of the cross section on Q^2 had been investigated for some cases up to $Q^2 = 9 \text{ GeV}^2$. We found that with increasing Q^2 the sum of the NLO resolved and the NLO direct cross section, in which the terms already contained in the resolved part were subtracted, approached the unsubtracted direct photon cross section. However, some difference remained even at the highest studied Q^2 . In NLO we expect reduced scale dependence of the predictions, in particular, when also the resolved cross section is calculated also up to NLO.

2 NLO Calculation of Jet Cross Sections

The NLO calculations are performed with the phase space slicing method. As is well known the higher order (in α_s) contributions to the direct and resolved cross sections have infrared and collinear singularities. To cancel them we use the familiar techniques. The singularities in the virtual and real contributions are regularized by going to d dimensions. In the real contributions the singular regions are separated with the phase-space slicing method based on invariant mass slicing. This way, we have for both, the direct and the resolved cross section, a set of two-body contributions and a set of three-body contributions. Each set is completely finite, as all singularities have been canceled or absorbed into PDF's. Each part depends separately on the phase-space slicing parameter y_s . The analytic calculations are valid only for very small y_s , since terms $O(y_s)$ have been neglected in the analytic integrations. For very small y_s , the two separate pieces have no physical meaning. The y_s is just a technical parameter which must be chosen sufficiently small and serves the purpose to distinguish the phase space regions, where the integrations are done analytically, from those, where they are performed numerically. The final result must be independent of the parameter y_s . In the real corrections for the direct cross section there are final state singularities and contributions from parton initial state singularities (from the proton side). This describes the calculation of the NLO cross section for the full direct cross section as well as for the NLO resolved cross section.

The resulting NLO corrections to the direct process become singular in the limit $Q^2 \rightarrow 0$, i.e. direct production with real photons. For $Q^2 = 0$ these photon initial state singularities are usually also evaluated with the dimensional regularization method. Then the singular contributions appear as poles in $\epsilon = (4 - d)/2$ multiplied with the splitting function $P_{q\gamma}$ and have the form $-\frac{1}{\epsilon}P_{q\gamma}$ multiplied with the LO matrix elements for quark-parton scattering [1]. These singular contributions are absorbed into PDF's $f_{a/\gamma}(x)$ of the real photon. For $Q^2 \neq 0$ the corresponding contributions are replaced by

$$-\frac{1}{\epsilon}P_{q\gamma} \rightarrow -\ln(s/Q^2)P_{q\gamma} \quad (1)$$

where \sqrt{s} is the c.m. energy of the photon-parton subprocess. These terms are finite as long as $Q^2 \neq 0$ and can be evaluated with $d = 4$ dimensions. For small Q^2 , these terms become large, which suggests to absorb them as terms proportional to $\ln(M_\gamma^2/Q^2)$ in the PDF of the virtual photon, which is present in the resolved cross section. M_γ is the factorization scale of the virtual photon. By this absorption the PDF of the virtual photon becomes dependent on M_γ^2 , in the same way as in the real photon case, but in addition it depends also on the virtuality Q^2 . Of course, this absorption of large terms is necessary only for $Q^2 \ll M_\gamma^2$. In all other cases the direct cross section can be calculated without the subtraction and the additional resolved contribution. M_γ^2 will be of the order

of E_T^2 . But also when $Q^2 \simeq M_\gamma^2$, we can perform this subtraction. Then the subtracted term will be added again in the resolved contribution, so that the sum of the two cross sections remains unchanged. This way also the dependence of the cross section on M_γ^2 must cancel, as long as we restrict ourselves to the resolved contribution in LO only. The cross section with the subtractions in the NLO corrections to the direct process will be denoted in the following the subtracted direct cross section. It is clear that this cross section alone has no physical meaning. Only with the resolved cross section added it can be compared with experimental data.

In the general formula for the deep-inelastic scattering cross section, one has two contributions, the transverse ($d\sigma_{\gamma b}^U$) and the longitudinal part ($d\sigma_{\gamma b}^L$). Since only the transverse part has the initial-state collinear singularity we have performed the subtraction only in the matrix element which contributes to $d\sigma_{\gamma b}^U$. Therefore we do not need the longitudinal PDF's $f_{a/\gamma}^L$. It is also well known that $d\sigma_{\gamma b}^L$ vanishes for $Q^2 \rightarrow 0$. The calculation of the resolved cross section including NLO corrections proceeds as for real photoproduction at $Q^2 = 0$ [1], except that the cross section is calculated also for final state variables in the virtual photon-proton center-of-mass system.

The invariant mass resolution mentioned above is not suitable to distinguish two and three jets in the final state. With the enforced small values for y_s the two-jet cross section would be negative in NLO, i.e. unphysical. Therefore one chooses a jet definition that enables one to define much broader jets. This is done in accordance with the jet definition in the experimental analysis by choosing the jet definition of the Snowmass meeting [19], where two partons are considered as two separate jets or as a single jet depending on whether they lie outside or inside a cone in the (η, ϕ) -plane with radius R around the jet momentum. The cone parameter R is chosen as in the experimental analysis, in the following $R = 1$. In NLO, the final state consists of two or three jets.

3 Parton Distributions of the Virtual Photon

For the computation of the direct and resolved components in the one- and two-jet cross sections we need the PDF's of the proton $f_{b/P}(x)$ and of the photon $f_{a/\gamma}(x)$ at the respective factorization scales M_P and M_γ . For the proton PDF's we have chosen the CTEQ4M version [20]. The factorization scales are put equal to the renormalization scale μ ($M_\gamma = M_P = \mu$), where μ will be specified later. For $f_{a/\gamma}$, the PDF of the virtual photon, we have chosen one of the parametrizations of Schuler and Sjöstrand (SaS) [16]. These sets are given in parametrized form for all scales M_γ , so that they can be applied without repeating the computation of the evolution. Unfortunately, these sets are given only in LO, i.e. the boundary conditions for $Q^2 = M_\gamma^2$ and the evolution equations are in LO. In [15] PDF's for virtual photons have been constructed in LO and NLO. However, parametrizations of the M_γ evolution have not been worked out. Second, these PDF's are only for $N_f = 3$ flavours, so that the charm and bottom contributions must be added as an extra contribution. Therefore we have selected a SaS version which includes charm and bottom as massless flavours. We defined the subtraction of the collinear singularities for the NLO direct cross section in the $\overline{\text{MS}}$ factorization. This has the consequence that, in addition to the dominant logarithmic term, also terms (in the limit $Q^2 = 0$) are left over in the NLO corrections of the subtracted direct cross section (see [8] for further details). To be consistent we must use a parametrization of the photon PDF that is defined in the $\overline{\text{MS}}$ factorization. In [16] such PDF's in the $\overline{\text{MS}}$ scheme are given in addition to

the PDF's in the DIS scheme, where the finite parts are put equal to zero. Actually, this distinction is relevant only in the NLO descriptions of the photon structure function. Since numerically, however, it makes a nonnegligible difference, whether one uses DIS or $\overline{\text{MS}}$ type PDF's of the photon the authors of [16] have presented both types of PDF's. Unfortunately, the $\overline{\text{MS}}$ version of [16] is defined with the so-called universal part of the finite terms, adopted from [21]. This does not correspond to the $\overline{\text{MS}}$ subtraction as we have used it in [8]. Therefore we start with the SaS1D parametrization in [16], which is of the DIS type with no finite term in $F_2^\gamma(x, M_\gamma^2)$ and transform it with the well-known formulas to the usual $\overline{\text{MS}}$ version. The heavy quarks c and b are included as massless flavours except for the starting scale Q_0 , which is $Q_0 = 600$ MeV for the u, d, s quarks and the gluon and related to the c and b quark masses, respectively.

All the existing PDF's of the virtual photon are theoretical constructions, which have not been tested or fitted to independent data from photon-photon scattering with a deep inelastic photon of large virtuality which corresponds to the factorization scale M_γ in our application and a photon with a moderate virtuality (target photon) which correspond to the Q^2 in our photoproduction case. In order to do this we have to wait for data from LEP. The few points measured by the PLUTO collaboration [17] were reproduced by the NLO PDF's of ref. [15], which is unfortunately not available in parametrized form. Actually the PLUTO measurement was only for $Q^2 = 0.35 \text{ GeV}^2$, which is not very much for testing the Q^2 dependence. In [5, 15, 16] the PDF's are constructed in such a way that they approach the PDF's for real photons in the limit $Q^2 \rightarrow 0$. The real photon PDF's have been compared to many data for F_2^γ , so that the x -dependence is constrained. The Q^2 dependence, however, is still untested and depends on assumptions, in particular in connection with the hadronic part. It is clear that for the larger Q^2 this is not relevant, since then the PDF is given essentially by the pointlike or anomalous part. This is shown in Fig. 1 (right), where we have plotted the u -quark part of the virtual photon PDF for $Q^2 = 10 \text{ GeV}^2$ and $M_\gamma^2 = 50 \text{ GeV}^2$. Here we compare the PDF of GRS [5] with the SaS version [16] and with the leading logarithmic singularity approximation which is identical to the subtraction term. As one can see these three functions coincide except at very small x , where the PDF is very small and in a small region around $x \simeq 1$. At smaller Q^2

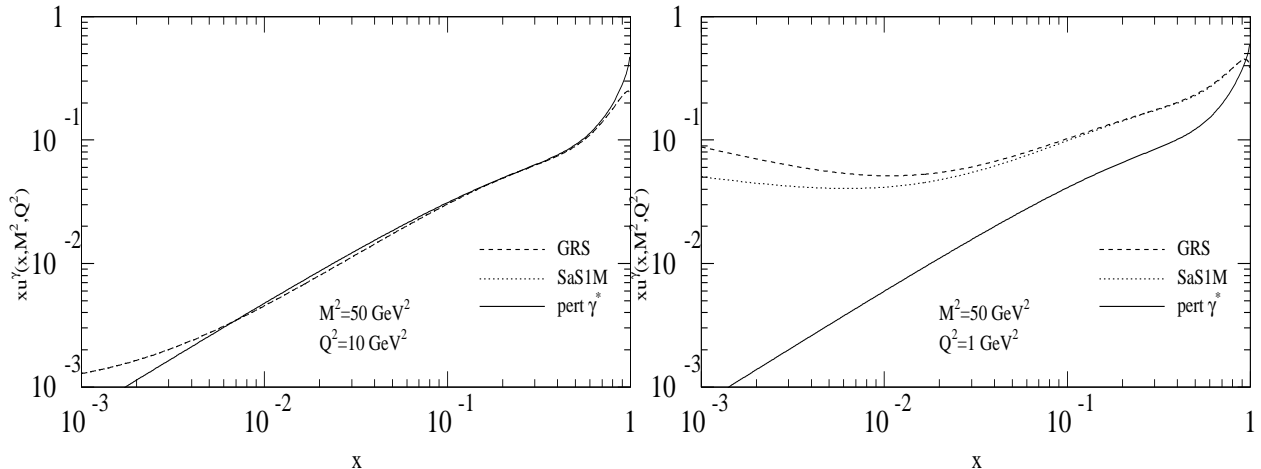


Figure 1: Comparison between the GRS and SaS1M LO predictions for the up-distribution of a virtual photon and the leading logarithmic singularity, denoted $\text{pert } \gamma^*$, in the $\overline{\text{MS}}$ scheme at the scale $M^2 = M_\gamma^2 = 50 \text{ GeV}^2$ for $Q^2 = 10.0 \text{ GeV}^2$ (left) and $Q^2 = 1.0 \text{ GeV}^2$ (right).

the situation is different. At $Q^2 = 1 \text{ GeV}^2$, which is shown in Fig. 1 (left), the two PDF's, GRS and SaS are very similar for the larger x , but differ very much from the logarithmic term.

4 Results

Here we shall show some numerical results in the form that we present first the full direct cross section including the transversal and the longitudinal part. Second, we have calculated the subtracted direct cross section and the resolved cross section which we superimpose to give the cross section which we compare with the full direct cross section. These results are given for the inclusive one-jet cross section, the exclusive two-jet rate and the inclusive two-jet cross section as a function of the rapidity η . The exclusive two-jet rate and the inclusive two-jet cross section will be compared with recent H1 data [13, 12]. For the purpose of the comparison with the exclusive two-jet data we have considered the Q^2 bins as shown in Tab. 1. In the experimental analysis only the bins II to VII are considered. We added the bin I in order to have results for cross sections of rather small virtuality, where the resolved part is more important than for all other bins. The bins chosen for the two-jet rate analysis of H1 involve some further cuts on the scattering angle and the energy of the electron in the final state. These are taken into account when we compare with the experimental data. For the more theoretical comparisons we have chosen simple cuts on the variable y , which is limited to the region $0.05 < y < 0.6$.

Of some importance is the choice of the scale μ . In bin I we have $Q^2 \ll E_T^2$, since in all considered cases $E_T > E_{T_{min}} > 5 \text{ GeV}$, so that $\mu = E_T$ would be a reasonable choice. Starting from bin V, $Q^2 \geq E_{T_{min}}^2$, so that from this bin on with the choice $\mu = E_T$ the resolved cross section would disappear at the minimal E_T and above up to $E_T^2 = Q^2$. In order to have a smooth behaviour for all E_T we have chosen $\mu^2 = Q^2 + E_T^2$, so that always $\mu^2/Q^2 > 1$ and in all bins a resolved cross section is generated. Of course, in the sum of the resolved and the subtracted direct cross section this scale dependence, which originates from the factorization scale dependence at the photon leg cancels to a very large extent in the summed cross section. Only the NLO corrections to the resolved cross section do not participate in the cancellation [22, 8].

Some characteristic results for the one-jet cross section as a function of Q^2 are shown in Fig 2 a, b, c and d. We have plotted the results for four selected bins I, II, V and VII. In these figures we show the rapidity distributions (the E_T distributions are found in [9])

$$\frac{d\sigma^{1jet}}{d\eta} = \int dE_T \frac{d^2\sigma^{1jet}}{dE_T d\eta} \quad , \quad (2)$$

where we have integrated the differential cross section over $E_T \geq 5 \text{ GeV}$.

Table 1: The seven subsequent bins of photon virtuality, Q^2 , considered in this work.

Bin number	I	II	III	IV	V	VI	VII
Q^2 -range in GeV^2	[1, 5]	[5, 11]	[11, 15]	[15, 20]	[20, 30]	[30, 50]	[50, 100]

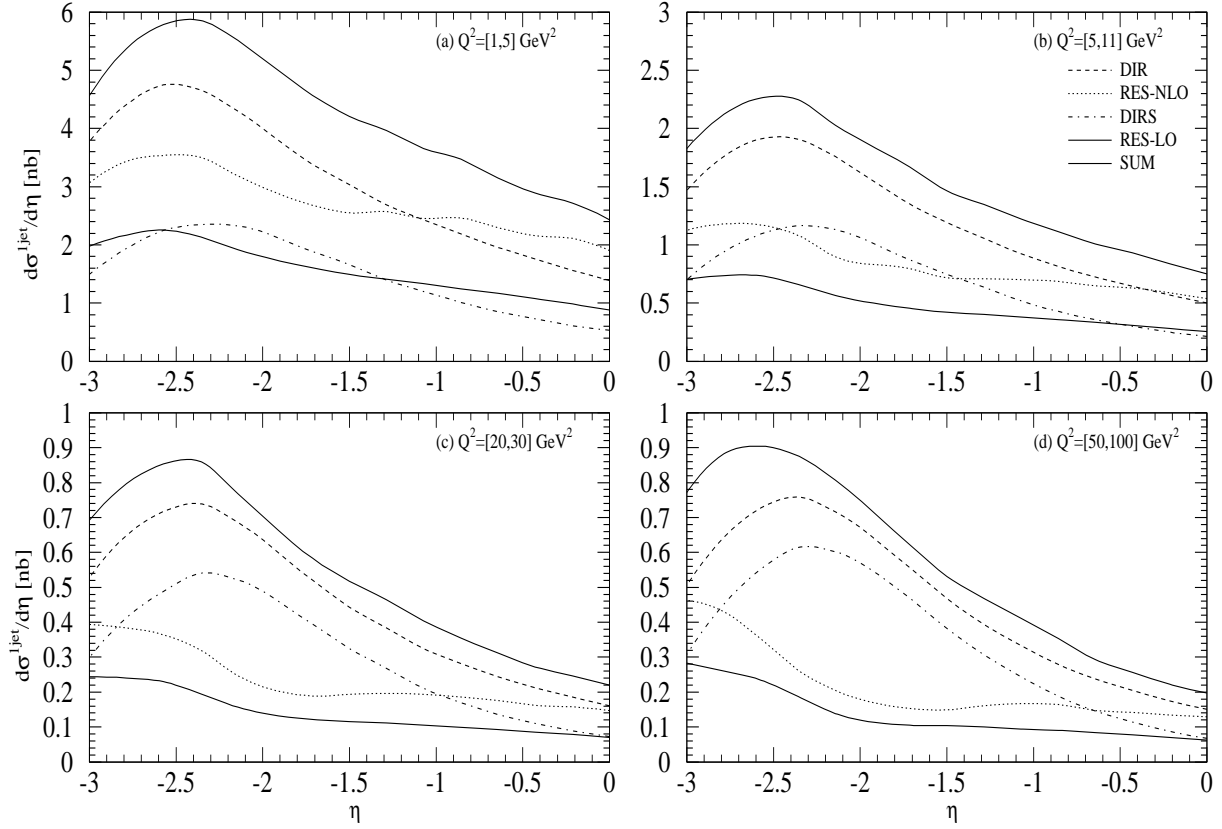


Figure 2: Inclusive single-jet cross section $d\sigma^{1jet}/d\eta$ integrated over $E_T > 5$ GeV as a function of η . In (a): $1 < Q^2 < 5$ GeV²; in (b): $5 < Q^2 < 11$ GeV²; in (c): $20 < Q^2 < 30$ GeV²; in (d): $50 < Q^2 < 100$ GeV². DIR stands for the NLO direct, DIRS is the NLO subtracted direct and RES-LO and RES-NLO are the LO and NLO resolved contributions, the lower full curve is always RES-LO, the upper one is SUM.

In the four plots we show five curves for $d\sigma^{1jet}/d\eta$ as a function of η in the range $-3 < \eta < 0$, since the cross section is significantly large only in the backward direction $\eta < 0$. η is the rapidity in the hadronic center-of-mass system. The five curves present the resolved cross sections (denoted by RES) in LO and NLO, the subtracted direct cross section denoted DIRS, the sum of DIRS and the NLO resolved cross section, denoted SUM in the figures, and the unsubtracted direct cross section labeled DIR. This cross section should be compared to the cross section, labeled SUM (upper full curve). As we can see, for all four Q^2 bins the DIR cross section is always smaller than the cross section obtained from the sum of DIRS and the NLO resolved cross section. Near the maximum of the cross sections they differ by approximately 25% in bin I and by 20% in the other bins. This means, at the respective Q^2 characterizing these bins, the summed cross section is always larger than the pure direct cross section. This difference originates essentially from the NLO corrections to the resolved cross section, as is obvious when we add the LO resolved curve to the DIRS contribution in Figs. 2 a, b, c and d. Up to a few percent the full DIR cross section and the LO resolved plus subtracted direct cross section are equal, except at the lowest Q^2 bins. This means that the term subtracted in the direct cross section is replaced to a very large extent by the LO resolved cross section. Differences between these two come from the evolution of the subtraction term to the scale $\mu = \sqrt{Q^2 + E_T^2}$ and contributions of the hadronic part at low Q^2 . This is to be expected

since at the considered values of $Q^2 > 1 \text{ GeV}^2$ the virtual photon PDF is essentially given by the anomalous (or point-like) part as shown in Fig. 1. All other contributions are of minor importance. Obviously the compensation of the LO resolved by the subtraction term is only possible, if the photon PDF is chosen consistently with the $\overline{\text{MS}}$ subtraction scheme, which is the case in our analysis. This also explains that the inclusion of the NLO corrections to the resolved cross section brings in additional terms and that the sum of DIRS and the NLO resolved part lies above the pure direct cross section. We conclude that except for the lowest two Q^2 bins, the NLO direct cross section gives approximately the same results as SUM, if we restrict ourselves to the LO contributions of the resolved cross section. Similar results for the inclusive dijet cross section are shown in [9]. The differential cross section $d^3\sigma/dE_T d\eta_1 d\eta_2$ yields the maximum of information possible on the parton distributions and is better suited to constrain them than with measurements of inclusive single jets.

We now come to the comparison with the exclusive two-jet rate R_2 as measured by H1 [13]. R_2 measures the cross section for two-jet production normalized to the total ep scattering cross section in the respective Q^2 bin. The data were obtained in the bins II to VII by requiring for both jets $E_T > 5 \text{ GeV}$ in the hadronic center-of-mass frame with the additional constraints $y > 0.05$, $k'_0 > 11 \text{ GeV}$ (k'_0 is the final state electron energy), $156^\circ < \theta_e < 173^\circ$ and integrated over η_1 and η_2 with $\Delta\eta = |\eta_1 - \eta_2| < 2$. Compared to the Q^2 bins considered in the previous sections, the H1 Q^2 bins are reduced through the additional constraints on k'_0 and the electron scattering angle θ_e . In the H1 analysis the two jets are searched for with the usual cone algorithm with $R = 1$ applied to the hadronic final state. In addition R_2 measures the exclusive two-jet rate, i.e. the contributions of more than two jets are not counted (here we discard remnant jets). Symmetric cuts $E_{T_1}, E_{T_2} \geq 5 \text{ GeV}$ are problematic from the theoretical viewpoint since the so defined cross section is infrared sensitive. With this same cut on the transverse energy of both jets there remains no transverse energy of the third jet, so that there is very little or no contribution from the three-body processes. Through the phase space slicing, needed to cancel infrared and collinear singularities in NLO, 3-body processes are always included inside the cutoff y_s , which, however, are counted in the $E_{T_1} = E_{T_2}$ contribution. For these contributions the y_s cut acts as a physical cut. In order to avoid this sensitivity on y_s one needs constraints on E_{T_1}, E_{T_2} or E_{T_3} which avoids the problematic region $E_{T_1} = E_{T_2}$. This problem was encountered already two years ago in the calculation of the inclusive two-jet cross section in photon-proton collisions [23].

A possibility to remove the infrared sensitivity is to require different lower limits on E_{T_1} and E_{T_2} , as for example,

$$E_{T_1}, E_{T_2} > 5 \text{ GeV}, \text{ and if } E_{T_1} > E_{T_2} \text{ (} E_{T_2} > E_{T_1} \text{) then } E_{T_1} > 7 \text{ GeV} \\ (E_{T_2} > 7 \text{ GeV}),$$

which we call the Δ mode. In this way, the third jet can have enough transverse energy to avoid the infrared sensitivity. Other cuts that also avoid the infrared region are possible but we will not discuss them here (see [9]). It is clear that the theoretical problems with the E_T cut on both jets appear equally in connection with NLO corrections to the direct as well as to the resolved cross section. The Δ mode has been considered also recently in connection with inclusive two-jet photoproduction in the HERA system [24].

Of course, the size of the dijet cross section depends on the way the cuts on E_{T_1} and E_{T_2} are introduced. Therefore, it is important that the same cuts are applied in the theoretical calculation and in the experimental analysis. The Δ mode, among others,

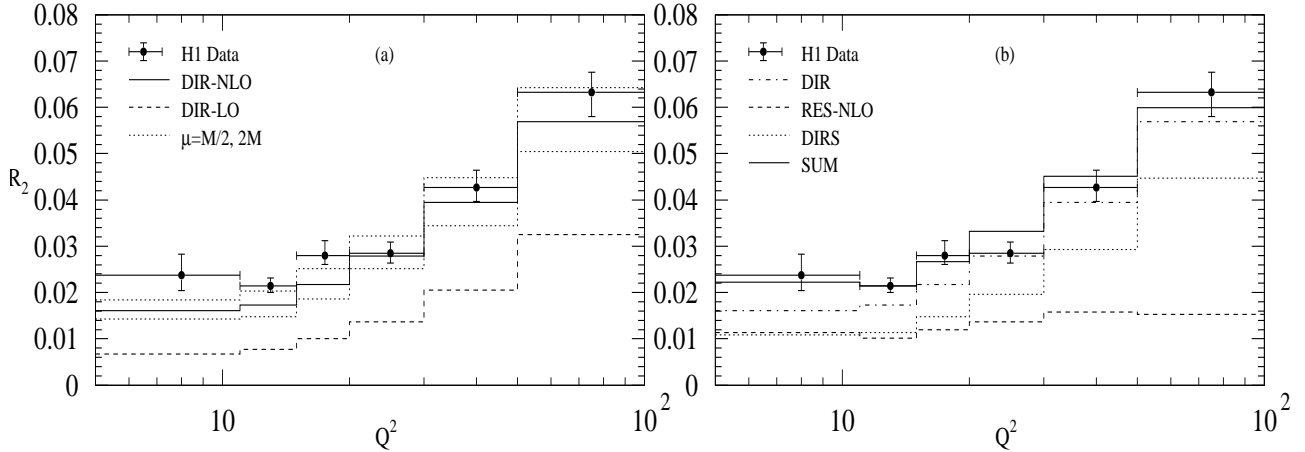


Figure 3: Dijet rate $R_2 = \sigma^{2jet}/\sigma^{tot}$ with $E_{T_{min}} = 5$ GeV for the Δ mode compared to H1-data. (a) The full line corresponds to the NLO deep-inelastic dijet rate (DIR-NLO), the dashed curve gives the LO deep-inelastic dijet rate (DIR-LO). The dotted lines show the scale variation for the NLO direct, where the upper dotted curve corresponds to the smaller scale. (b) The dash-dotted curve gives the NLO direct (DIR-NLO), the dashed is NLO resolved (RES-NLO), the dotted is NLO DIRS and the full is SUM.

has been applied also in the measurements of R_2 [13], so that for this mode our results can be compared directly to the data. This we do in Fig. 3. We compare results for the direct cross section in LO (DIR-LO) and NLO (DIR-NLO) for three different scales $\mu = M/2, M, 2M$ where $M = \sqrt{Q^2 + E_{T_1}^2}$, calculated for the Q^2 bins II to VII with the additional cuts on k'_0 and θ_e mentioned above. We see that the NLO corrections are appreciable. Since the scale μ is rather low we have to expect such large K factors. On the other hand the scale variation is moderate, so that we are inclined to consider the NLO cross section as a safe prediction. In Fig. 3 b we compare the NLO direct cross section (DIR) with the sum (SUM) of the subtracted direct (DIRS) and the NLO resolved cross section (RES-NLO) for the six Q^2 bins. In addition, we show the contribution of the two components (DIRS and RES-NLO) in the sum separately. In the first Q^2 bin, DIRS and the NLO resolved cross section are almost equal, the cross section in the largest Q^2 bin is dominated by DIRS. In this bin the unsubtracted direct cross section DIR is almost equal to the sum of DIRS and NLO resolved. In the first Q^2 bin this cross section is 50% larger than the NLO direct cross section. We also compare with the H1 data [13]. In the smaller Q^2 bins the sum of DIRS and NLO resolved agrees better with the experimental data than the DIR cross section. In the two largest Q^2 bins the difference of the cross sections DIR and SUM is small and it can not be decided which of these cross sections agrees better with the data due to the experimental errors. This is in contrast to the 30% difference between the DIR and SUM found for the inclusive single-jet cross sections in Fig. 2, which we attribute to the NLO corrections of the resolved contributions. This difference is reduced in the dijet rate R_2 due to the specific cuts on the transverse energies of the two jets in the definition of the dijet rate. These cuts suppress the resolved component stronger than the direct one, which leads to the observed behaviour of the dijet rate at the large Q^2 bins. We emphasize that the theoretical cross sections are calculated on parton level whereas the experimental two-jet rate is based on hadron jets. Corrections due to hadronization effects are estimated to be typically around 5% and at most 20% [13]. We finally mention that we have also compared NLO predictions with a different mode that

H1 Preliminary

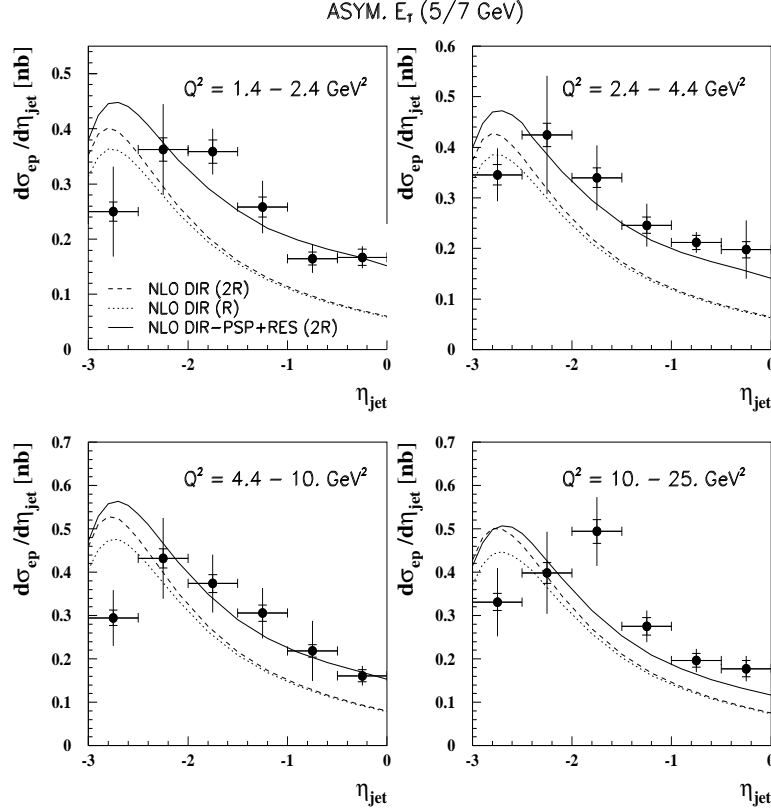


Figure 4: Dijet inclusive cross section $d\sigma_{ep}/d\eta_{jet}$ as a function of rapidity in the Δ mode compared to NLO direct (DIR) for two different R_{sep} parameters and the sum of NLO DIRS plus NLO resolved (calculated with JETVIP [9]).

avoids the infrared region and found similar results as those for the Δ mode (see [9] for details).

We come to a second analysis for dijet cross sections, presented in [12], which was also done in the hadronic center-of-mass frame. Jets were selected using the cone algorithm with $R = 1$. As before, the Δ mode was used to avoid infrared sensitive regions. Some additional cuts were imposed on the scattered electron (see [12]). The differential inclusive two-jet cross section $d\sigma/d\eta$ as a function of the rapidity for the four Q^2 bins $1.4 < Q^2 < 2.4 \text{ GeV}^2$, $2.4 < Q^2 < 4.4 \text{ GeV}^2$, $4.4 < Q^2 < 10. \text{ GeV}^2$ and $10. < Q^2 < 25. \text{ GeV}^2$ is shown in Figure 4. The full curve is the cross section obtained from the NLO resolved plus subtracted direct cross section. The two other curves (dashed and dotted) present two unsubtracted direct cross sections with two different choices of the R_{sep} parameter: $R_{sep} = R$ and $R_{sep} = 2R$. The latter choice corresponds to no R_{sep} parameter, which we had chosen also for all results presented so far. The influence of the R_{sep} parameter is small except at very negative η 's. The agreement between the data [12] and the NLO predictions is better when a resolved component is included, especially in the forward η region. We note that the agreement is even better, in particular for $\eta \simeq -3$, when corrections for hadronisation are applied [12].

5 Conclusions

We have reviewed the calculations of cross sections in NLO for inclusive single-jet and dijet production in low Q^2 ep scattering at HERA. The results of two approaches were compared as a function of Q^2 in the range $1 < Q^2 < 100 \text{ GeV}^2$. In the first approach the jet production was calculated in NLO from the usual mechanism where the photon couples directly to quarks. In the second approach the logarithmic dependence on Q^2 of the NLO corrections is absorbed into the parton distribution function of the virtual photon and the jet cross sections are calculated from the subtracted direct and the NLO resolved contributions. Over the whole Q^2 range considered in this work, this sum gives on average 25% larger single-jet cross sections than the usual evaluation based only on the direct photon coupling. This difference is attributed to the NLO corrections of the resolved cross sections. If these NLO corrections are neglected the sum of the subtracted direct and the LO resolved contributions agrees approximately with the unsubtracted direct cross sections.

We calculated also the dijet rate based on the exclusive dijet cross section and differential dijet distributions and compared it with recent H1 data. The dijet rate is plotted as a function of Q^2 , the rapidities and transverse energies are integrated with $E_T \geq 5 \text{ GeV}$. The dijet rate is sensitive to the way the transverse energies of the two jets are cut. If the cuts on the E_T 's are exactly at the same value the cross section is infrared sensitive. We showed results with one particular definition for the kinematical constraints on the transverse energies of the measured jets. The calculated and the measured two-jet rates agree quite well over the measured Q^2 range $5 < Q^2 < 100 \text{ GeV}^2$. In the lowest Q^2 bin only the dijet rate based on the sum of the subtracted direct and resolved cross sections agrees with the experimental value. Also the differential dijet cross sections as a function of rapidity agreed quite well with the predictions. The version of the theory including a resolved component was preferred by the data.

Acknowledgements

We thank M. Tasevsky for producing the NLO curves for Fig. 4 with JETVIP and for providing us with the plots including the H1 data. One of us (B.P.) thanks the organizers of the workshop for a pleasant and stimulating working atmosphere.

References

- [1] M. Klasen, T. Kleinwort, G. Kramer, Eur. Phys. J. direct C1 (1998) 1
- [2] For reviews see: J. Butterworth in Proceedings of the Ringberg Workshop, New Trends in HERA Physics, edited by B A Kniehl, G Kramer, A Wagner, World Scientific, Singapore, 1998, p. 225; S. Söldner-Rembold in 18th International Symposium on Lepton-Photon Interactions, LP'97, editors A. De Roeck and A. Wagner, World Scientific, Singapore, 1998, p. 97;
J. Breitweg et al., ZEUS Collab., Eur. Phys. J. C4 (1998) 591
- [3] E. Mirkes, D. Zeppenfeld, Phys. Lett. B380 (1996) 23; Acta Phys. Polon. B27 (1996) 1392; S. Catani, M.H. Seymour, Phys. Lett. B378 (1996) 287; Nucl. Phys. B485

- (1997) 291; D. Graudenz in Proceedings of the Ringberg Workshop, New Trends in HERA Physics, p. 146, PSI-PR-97-20, hep-ph/9709240
- [4] For a review see: T. Carli in Proceedings of the Ringberg Workshop, New Trends in HERA Physics, p. 129;
C. Adloff et al., H1 Collab., report DESY 98-075, June 1998, hep-ex/9806028; report Desy 98-087, July 1998, hep-ex/9807019
- [5] M. Glück, E. Reya, M. Stratmann, Phys. Rev. D54 (1996) 5515
- [6] D. de Florian, C. Garcia Canal, R. Sassot, Z. Phys. C75 (1997) 265
- [7] J. Chyla, J. Cvach, Proceedings of the Workshop 1995/96 on "Future Physics at HERA", eds. G. Ingelman, A. de Roeck, R. Klanner, DESY 1996, Vol. 1, p. 545
- [8] M. Klasen, G. Kramer, B. Pötter, Eur. Phys. J. C1 (1998) 261; B. Pötter, DESY 97-138, July 1997, hep-ph/9707319
- [9] G. Kramer, B. Pötter, report DESY 98-046, April 1998, hep-ph/9804352, Eur. Phys. J. C (in print), B. Pötter, report DESY 98-071, June 1998, hep-ph/9806437
- [10] C. Adloff et al., H1 Collab., Phys. Lett. B415 (1997) 418;
- [11] H1 Collab., subm. to the 29th Int. Conf. on HEP, ICHEP98, Vancouver, Canada, July 1998; S.J. Maxfield (H1 Collab.), these proceedings.
- [12] J. Chyla (H1 Collab.), talk at HERAMC Workshop, WG 30, October 1998
- [13] C. Adloff et al., H1 Collab., report Desy 98-076, June 1998, hep-ex/9806029
- [14] N. Macdonald (ZEUS Collab.), talk at the HERAMC Workshop, WG 30, October 1998; C. Foudas (ZEUS Collab.), talk given at the Int. Conf. on QCD, Montpellier, France, July 1998.
- [15] M. Glück, E. Reya, M. Stratmann, Phys. Rev. D51 (1995) 3220
- [16] G.A. Schuler, T. Sjöstrand, Z. Phys. C68 (1995) 607, Phys. Lett. B376 (1996) 193
- [17] Ch. Berger et al., PLUTO Collab., Phys. Lett. B142 (1984) 119
- [18] F.M. Borzumati, G.A. Schuler, Z. Phys. C58 (1993) 139
- [19] J.E. Huth et al., Proc. of the 1990 DPF Summer Study on High Energy Physics, Snowmass, Colorado, edited by E.L. Berger, World Scientific, Singapore, 1992, p. 134.
- [20] H.L. Lai, J. Huston, S. Kuhlmann, F. Olness, J. Owens, D. Soper, W.K. Tung, H. Weerts, Phys. Rev. **D55** (1997) 1280.
- [21] P. Aurenche, M. Fontannaz, J.-Ph. Guillet, Z. Phys. **C64** (1994) 621.
- [22] D. Bödeker, G. Kramer, S.G. Salesch, Z. Phys. C63 (1994) 471.
- [23] M. Klasen, G. Kramer, Phys. Lett. B366 (1996) 385.
- [24] S. Frixione, G. Ridolfi, Nucl. Phys. B507 (1997) 315.